Cannabidiol protects C2C12 myotubes against cisplatin-induced atrophy by regulating oxidative stress

Olivier Le Bacquer, Phelipe Sanchez, Véronique Patrac, César Rivoirard, Nicolas Saroul, Christophe Giraudet, Ayhan Kocer, Stéphane Walrand

Cannabidiol protects C2C12 myotubes against cisplatin-induced atrophy by regulating oxidative stress

Running title: CBD prevents cisplatin-induced muscle atrophy in vitro

Olivier Le Bacquer[1], Phelipe Sanchez[1], Véronique Patrac[1], César Rivoirard[1], Nicolas Saroul[1,2], Christophe Giraudet[1], Ayhan Kocer[3], Stéphane Walrand[1,4]

1. Unité de Nutrition Humaine (UNH), Université Clermont Auvergne, INRAE, CRNH Auvergne, 63000 Clermont-Ferrand, France.
2. Department of Head and Neck Surgery, Clermont-Ferrand University Hospital, Clermont-Ferrand, France.
3. Université Clermont Auvergne, iGReD, CNRS UMR 6293, INSERM U1103, 28, place Henri Dunant, BP38, 63001 Clermont-Ferrand, France.
4. CHU Clermont-Ferrand, Service Nutrition Clinique, 63000 Clermont-Ferrand, France.

*correspondence to: Olivier Le Bacquer, Ph.D.

INRAE, UMR1019, Université Clermont Auvergne, UNH - Unité de Nutrition Humaine, CRNH Auvergne, 63000 Clermont-Ferrand, France.
Phone: +33 473178248 / fax: +33 473178222
Email: olivier.le-bacquer@inrae.fr
ORCID : 0000-0003-3805-973X

Supplemental data available at :
URL : https://figshare.com/articles/figure/Supplemental_Figure_S1-AJPCellPhysiol_2024_pdf/25196435
DOI : https://doi.org/10.6084/m9.figshare.25196435

ABSTRACT

Cancer and chemotherapy induce a severe loss of muscle mass (known as cachexia), which negatively impact cancer treatment and patient survival. The aim of the present study was to investigate whether CBD administration may potentially antagonize the effects of cisplatin in inducing muscle atrophy, using a model of myotubes in culture. Cisplatin treatment resulted in a reduction of myotube diameter (15.7±0.3 vs. 22.2±0.5 µm, $p<0.01$) that was restore to control level with 5µM CBD (20.1±0.4 µM, $p<0.01$). Protein homeostasis was severely altered with a ≈70% reduction in protein synthesis ($p<0.01$) and a 2-fold increase in proteolysis ($p<0.05$) in response to cisplatin. Both parameters were dose dependently restored by CBD co-treatment. Cisplatin treatment was associated with increased TBARS content (0.21±0.03 to 0.48±0.03 nmol/mg prot, $p<0.05$), catalase activity (0.24±0.01 vs. 0.13±0.02 nmol/min/µg prot, $p<0.01$), whereas CBD co-treatment normalized TBARS content to control values (0.22±0.01 nmol/mg prot, $p<0.01$) and reduced catalase activity (0.17±0.01 nmol/min/µg prot, $p<0.05$). These changes were associated with increased mRNA expression of GPX1, SOD1, SOD2 and CAT mRNA expression in response to cisplatin ($p<0.01$), which was corrected by CBD co-treatment ($p<0.05$). Last, cisplatin treatment increased the mitochondrial protein content of NDUFB8, UQCRC2, COX4 and VDAC1 (involved in mitochondrial respiration and apoptosis), and CBD co-treatment restore their expression to control values. Altogether, our results demonstrated that CBD antagonize the cisplatin-induced C2C12 myotube atrophy and could be used as an adjuvant in the treatment of cancer cachexia to help maintain muscle mass and improve patient quality of life.

New and noteworthy: In an in vitro model, cisplatin treatment led to myotube atrophy associated with dysregulation of protein homeostasis and increased oxidative stress, resulting in increased apoptosis. Co-treatment with cannabidiol was able to prevent this phenotype by promoting protein homeostasis and reducing oxidative stress.

KEYWORDS

cachexia, endocannabinoid system, protein homeostasis, oxidative stress, mitochondrial function

INTRODUCTION

Cachexia is a multifactorial wasting syndrome characterized by a severe involuntary loss of body weight (i.e. more than 5% body weight loss in the last 12 months or less), loss of skeletal muscle mass (with or without loss of fat mass), anorexia, and dysregulated energy and protein metabolism (1). Prevalence of cachexia varies with cancer type, from 15% in prostate cancer up to 60% in pancreatic cancer (2). Several studies have clearly demonstrated that survival times are shorter in patients who have experienced weight loss than in those who have not. Weight loss is not only predictive of survival but also of response to chemotherapy (3). One of the mechanisms that has been advanced to explain why patients with cachexia have poorer survival is their higher incidence of complications related to surgical, radiotherapeutic and chemotherapeutic treatments (4). Cachexia is associated with increased fatigue and frailty, reduced physical activity leading to loss of autonomy, and decreased quality of life (5, 6). In some cases, the impact of cachexia is severe enough to necessitate chemotherapy dose reductions, treatment postponements or permanent discontinuation, in which case patients who lose weight do not get the full potential benefit of their cancer therapy (4, 7). Maintaining skeletal muscle mass in cancer patients is therefore crucial to their management, improved response to associated therapies, and improved quality of life. There are no formal guidelines for the management of cancer-related muscle wasting, but an effective strategy should aim to reduce muscle wasting in order to promote survival in patients with advanced cancer (8). One straightforward way to do this is through nutrition (9).

Cancer treatment often involves chemotherapy, which itself contributes to the development and progression of muscle atrophy and weakness in treated patients and preclinical models (10-13). Chemotherapy has been found to reduce muscle mass index and strength in lung and breast cancer patients (10), and cisplatin treatment in head and neck cancer patients decreased muscle strength measured by chair-lift and arm flexion tests (11). This same type of muscle dysfunction is also observed in preclinical models of cancer and chemotherapy. For example, in mice, implantation of C26 colonic tumor or lung carcinoma led to muscle atrophy associated with a decrease in mitochondrial respiration (14) and an alteration of the processes regulating mitochondrial biogenesis and dynamics (fusion/fission) (15). Similarly, treatments using cisplatin or doxorubicin, two widely-used chemotherapy agents, increased muscle mitochondrial dysfunction by altering mitochondrial biogenesis and dynamics (16-18). These data are consistent with the mitochondrial dysfunction, decreased mitochondrial content, and alterations in mitochondrial dynamics that are well-documented in cancer patients (19). As a

result, damaged mitochondria accumulate in skeletal muscle and, in addition to being less bioenergetically efficient, promote oxidative stress through increased production of reactive oxygen species (ROS). In mice, administration of doxorubicin or cisplatin leads to an increase in ROS production (16-18). Mitochondrial dysfunction and increased oxidative stress disrupt protein turnover pathways, leading to decreased protein synthesis and increased activity of muscle proteolytic systems (proteasome, autophagy) (12, 20), ultimately resulting in muscle fiber atrophy (16, 17).

The endocannabinoid system is a major molecular system responsible for controlling metabolism throughout the body, and is becoming an increasingly popular target for pharmacotherapy. Endocannabinoids (EC) and phytocannabinoids are the two main subclasses of cannabinoids. EC are produced by mammals, whereas phytocannabinoids, including cannabidiol (CBD), are produced by plants such as *Cannabis sativa* (21). EC exert their pharmacological effects via the endogenous endocannabinoid system, mainly by interacting with various receptors, primarily CB1 and CB2 (21). CBD is a weak agonist of CB1 and CB2, and can activate multiple cellular targets (e.g. TRPV1, PPARγ) or inhibit (e.g. GPR55) (22). The EC system is involved in numerous physiological processes, such as memory, appetite, and the regulation of metabolic energy balance (21). EC exert a central effect by stimulating food intake but also by modulating lipid and carbohydrate metabolism in the liver, adipose tissue and skeletal muscle to favor energy accumulation (21). There is also growing evidence that the EC system and CBD plays an important role in regulating mitochondrial biogenesis, membrane integrity and oxidative capacity (23). Our laboratory and other teams have demonstrated that the EC system also controls muscle development (24, 25) and that alterations in the EC system are associated with muscle dysfunction (26-29). The use of CBD could therefore hold benefit for improving the treatment of cancer and cancer-induced cachexia, in particular by protecting skeletal muscle mass.

Recent studies have shown that CBD has antineoplastic and anti-inflammatory properties in numerous in vitro models (30). Recent evidence also indicates that CBD regulates oxidative activity and mitochondrial content in the myocardium by modulating the expression of several markers of mitochondrial biogenesis that had been severely reduced by doxorubicin treatment (13). In addition to its effects on mitochondria, CBD also has beneficial effects on skeletal muscle. In mdx mice, i.e. a model of Duchenne muscular dystrophy, Iannotti *et al.* reported that CBD was able to prevent loss of motor activity by promoting myotube formation and reducing

inflammation (27). CBD also reduces the production of ceramides (deleterious lipid derivatives responsible for mitochondrial dysfunction) in high-fat diet-induced obesity (31).

Taken together, these data show that there is currently no treatment to prevent or reduce cachexia, and that CBD could be a promising candidate compound for use as an adjuvant in cancer treatment, due to its demonstrated positive effects on mitochondrial function, oxidative stress, and skeletal muscle development, metabolism and. Here, we used a model of myotubes in culture to investigate whether CBD treatment was able to counteract the muscle atrophy induced by chemotherapy (cisplatin).

MATERIAL AND METHODS

Chemicals and reagents. Dulbecco's modified Eagle medium (DMEM) and phosphatase inhibitor cocktail were purchased from Sigma-Aldrich (Saint-Quentin-Fallavier, France). Fetal bovine serum, horse serum, trypsin-EDTA, PBS, and penicillin-streptomycin were purchased from PAA (Pasching, Austria). Primary antibodies were obtained from the following sources. Thr389-phosphorylated S6K (#34475, 1/1000) total S6K (#9202, 1/1000), Ser473-phosphorylated Akt (#9271, 1/1000), total Akt (#9272, 1/1000), Ser51- phosphorylated eIF2α (#3398, 1/1000), total eIF2α (#5324, 1/1000), Thr172-phosphorylated AMPK (#2535, 1/1000), total AMPK (#2532, 1/1000), caspase 3 (#9662, 1/1000), and VDAC (#4866, 1/1000) antibodies were from Cell Signaling Technology (distributed by Ozyme, Saint-Quentin-en-Yvelines, France). Mouse anti-puromycin mAb (clone 12D10) (#MABE343, 1/1000) was from Sigma-Aldrich (Saint-Quentin-Fallavier, France). Horseradish peroxidase-conjugated secondary antibodies were from DAKO (Trappes, France). GAPDH antibody (#9545, 1/5000) was from Sigma-Aldrich (Saint-Quentin-Fallavier, France). Polyubiquitin antibody (#ENZ-ABS840-0100, 1/1000) was purchased from Enzo Life Sciences (Villeurbanne, France). Total OXPHOS antibody (#MS604, 1/1000) was purchased from Mitosciences (Eugene, Oregon, USA). CoxIV antibody (#MA5-31470, 1/1000) was from Thermo Fisher Scientific (Courtaboeuf, France). Cisplatin and cannabidiol and the TBARS and catalase assay kits were purchased from Cayman Chemicals (distributed by INTERCHIM, Montluçon, France).

Cell culture and differentiation. Mouse C2C12 myoblasts cells were purchased from the ATCC (#CRL-1772, American Type Culture Collection; Manassas, VA). Myoblasts were cultured in a growth medium composed of DMEM containing 4.5 g/L glucose, 2.4 g/L sodium bicarbonate, 10% fetal bovine serum, 100 UI/mL penicillin, and 0.1 mg/mL streptomycin, and incubated at 37°C in humidified air with 5% CO_2. The medium was changed every other day to ensure growth until 90% confluence. Myotube formation was induced by changing the growth medium to a differentiation medium consisting of DMEM supplemented with 2% horse serum, 100 UI/mL penicillin, and 0.1 mg/mL streptomycin for 5 days before cell treatment. Passages between 4 and 10 were used for the experiments.

Cell treatments. For all experiments, C2C12 cells were incubated in differentiation medium. Cisplatin was prepared extemporaneously in PBS to obtain a 0.5 mg/mL stock solution, then administered to the cells at a final concentration of 50 µM for 24–48 h. A stock solution of CBD was prepared in ethanol and stored at -80°C. For each experiment, cells were pre-treated for 2 h prior to cisplatin treatment with CBD concentrations corresponding to those used in

subsequent cisplatin conditions (ranging from 1 to 5µM of CBD). After this pre-treatment, cells were incubated with cisplatin with or without a CBD concentration corresponding to the pre-treatment CBD concentration. Control experiments were conducted with the equivalent amount of PBS and ethanol used in the cisplatin and CBD settings. C2C12 viability was estimated using the CellTiter-Glo® luminescent assay (Promega, France).

C2C12 myotube morphology analysis. Myotubes were photographed directly in the culture plates without fixation, using an AxioCam ERc5s digital camera coupled to an AxioVert.A1 microscope and ZEN 2.3 software (Zeiss, Germany). Myotube diameter was measured from three independent experiments on myotubes in each condition. Three random measurements were performed along the length of each myotube (n=3 measurements/myotube) using the ZEN 2.3 software, and the average of the three measures was considered as a single value.

Western blotting and measurement of protein synthesis rate. Protein synthesis was assessed according to the SUnSET method. The SUnSET technique uses puromycin, which incorporates into nascent polypeptide chains and terminates the elongation, resulting in an accumulation of puromycin-conjugated peptides that reflects the rate of protein synthesis. Briefly, C2C12 cells were incubated with 1 µM puromycin for the last 30 min of experimental treatments, then washed twice with ice-cold PBS and homogenized in ice-cold buffer (50 mM HEPES pH 7.4, 150 mM NaCl, 10 mM EDTA, 10 mM NaPPi, 25 mM β-glycerophosphate, 100 mM NaF, 2 mM Na orthovanadate, 10% glycerol, 1% Triton X-100) containing 1% protease inhibitor cocktail (Sigma-Aldrich, Saint-Quentin-Fallavier, France). Homogenates were centrifuged at 13,000 × *g* for 10 min at 4°C. Denatured proteins were separated by SDS-PAGE and transferred to a PVDF membrane (Millipore, Molsheim, France). Immunoblots were blocked with 0.1% TBS-Tween-20 containing 5% dry milk, and then probed overnight at 4°C with primary antibodies. After several washes with 0.1% TBS-Tween-20, the immunoblots were incubated with a horseradish peroxidase-conjugated secondary antibody (DAKO, Trappes, France) for one hour at room temperature. Immune-reactive bands or whole lanes were visualized by chemiluminescence (ECL Western blotting substrate, Thermo Fisher Scientific, Courtaboeuf, France). escent secondary antibodies were visualized using an MF-ChemiBIS 2.0 camera (Fusion Solo, Vilber Lourmat, France). Band densities were quantified using MultiGauge 3.2 software (Fujifilm Corporation, FSVT, Courbevoie, France). An internal control was used on each gel to normalize signal intensities between gels.

RNA extraction and quantitative real-time PCR. Total RNA was extracted using Trizol reagent (Invitrogen) according to the manufacturer's instructions. RNA was quantified by

measuring optical density at 260 nm. The concentrations of the mRNAs corresponding to genes of interest were measured by reverse transcription followed by real-time PCR using an AriaMX Real-Time PCR System (Agilent, Les-Ulis, France). One microgram of total RNA was reverse-transcribed using SuperScript® III reverse transcriptase and a combination of random hexamer and oligo-dT primers (Invitrogen). PCR amplification was performed in a 20 µL total reaction volume. The real-time-PCR mixture contained 5 µL of diluted cDNA template, 10 µL of 2x ONE Green® Fast qPCR premix (Ozyme, Saint-Cyr-l'École, France), and 0.5 µM of forward and reverse primers. The amplification profile was initiated by 3 min incubation at 95°C to activate the hot-start Taq DNA Polymerase, followed by 40 cycles of two steps: 95°C for 5 sec (denaturation step) and 60°C for 30 sec (annealing/extension step). Relative mRNA concentrations were analyzed using the AriaMX software. Relative mRNA abundance was calculated using the 2-ΔΔCT method with 18S as housekeeping gene. Mitochondrial DNA (mtDNA) was quantified by measuring the ratio between the expression of mitochondrial ND1 DNA and nuclear actin DNA as reference. Details of the primers used in the PCR can be found in table 1.

Statistical analysis. Data are expressed as mean ± SE. Between group differences were analyzed using one-way ANOVA and Tukey's test for post hoc comparisons. Statistical significance was set at $P < 0.05$ for all analyses.

RESULTS

CBD prevents cisplatin-induced C2C12 myotube atrophy and death. In a first set of experiments, we studied whether CBD was able to prevent the atrophy of C2C12 myotubes in response to cisplatin treatment. In absence of CBD, cisplatin induced myotube atrophy, as exemplified by a ≈30% reduction (p<0.01) in myotube diameter (Fig. 1A,B). However, co-treatment with CBD prevented myotube atrophy in a dose-dependent manner (Fig. 1A, B). As muscle morphology analysis revealed a high degree of cell death in response to cisplatin (Fig. 1A), we measured ATP content as an index of cell viability. We observed that myotube viability was marginally affected by cisplatin and CBD after 24 h of treatment (data not shown) but was reduced by ≈30% after 48 h of treatment (Fig. 1C). CBD restored myotube viability in a dose-dependent manner, reaching full protection at a 3 µM concentration (Fig. 1C). Western blot analysis revealed that the reduction in cell viability observed in response to cisplatin was associated with the appearance of the cleaved form of caspase 3 indicating induction of apoptosis (Fig. 1D,E). Similar results were observed in myoblast (supplemental figure). As expected, CBD treatment prevented the apoptotic process, as evidenced by the dose-dependent reduction in protein expression of the cleaved-caspase 3 (Fig. 1D,E).

CBD restores protein homeostasis in cisplatin-treated C2C12 myotubes. To investigate whether cisplatin alters protein synthesis and proteolysis and whether CBD is able to counteract this effect, we incubated C2C12 myotubes for 24 h in differentiation media in the presence of cisplatin and increasing concentrations of CBD, and then measured protein synthesis using the SUnSET technique. As shown in Fig. 2A and B, puromycin incorporation was reduced by ≈75% (p<0.01) in response to cisplatin treatment. Protein synthesis is mainly controlled by the Akt/mTOR/S6K and eIF2α signaling pathways, where anabolic conditions lead to increased phosphorylation of Akt on Ser473 and S6K on Thr389 and decreased phosphorylation of eIF2α on Ser51 residue. As shown in Fig. 2A, C-E, cisplatin treatment was associated with decreased phosphorylation of both Akt and S6K and increased phosphorylation of eIF2α, in agreement with the observed reduced protein synthesis. Co-treatment with CBD was able to restore protein synthesis (Fig. 2A, B), which was associated with a dose-dependent increase in Akt phosphorylation on Ser473 and S6K phosphorylation on Thr389, and a dose-dependent decrease of Ser51 phosphorylation on eIF2α (Fig. 2A, C-E). AMPK kinase is activated by an elevated AMP/ATP ratio due to cellular and environmental stress. We observed that cisplatin treatment was associated with an increase in AMPK phosphorylation on Thr172 that was

corrected by CBD co-treatment (Fig. 2A). To investigate how cisplatin and cannabidiol impact proteolysis, we evaluated the level of protein poly-ubiquitination and the mRNA expression of MAFBx and MuRF1. As shown in Fig. 3A,B, cisplatin treatment increased protein polyubiquitination by ≈70% (p<0.01) and induced a ≈2-fold increase in mRNA expression of Atrogin1/MAFBx (Fig. 3C) and MuRF1 (Fig. 3D). CBD reduced protein polyubiquitination levels in a dose-dependent manner (Fig. 3A,B), and CBD treatment at a 5 µM concentration restored the mRNA expression of both Atrogin1/MAFBx and MurF1 to control levels (Fig. 3C,D).

CBD prevents cisplatin-induced oxidative stress in C2C12 myotubes. The toxicity of cisplatin has been described as a function of DNA binding followed by single-stranded DNA breaks. More recently, cisplatin has been shown to generate oxidative stress, which can also contribute to its anti-tumor effects (32). To determine whether cisplatin-induced C2C12 myotube atrophy was associated with oxidative stress, we measured the level of TBARS, a marker of lipid peroxidation, in C2C12 myotubes in response to cisplatin and CBD treatments. We found a two-fold increase in TBARS content in response to 24 h cisplatin treatment that was prevented by co-treatment with 5 µM CBD (Fig. 4A). Catalase is one of the main enzymes responsible for the detoxification of hydrogen peroxide, a reactive oxygen species. We therefore measured catalase activity in response to cisplatin and CBD treatments (Fig. 4B). A 24 h cisplatin treatment induced a ≈90% increase in catalase activity, indicating severe oxidative stress (0.236 ± 0.020 *vs* 0.125 ± 0.013 nmol/min/µg prot, p<0.01) that was partially restored by co-treatment with CBD (0.172 ± 0.010 vs 0.236 ± 0.020 nmol/min/µg prot, p<0.05). We then measured the mRNA expression levels of several anti-oxidant systems. As shown in Fig. 4C, mRNA expression of GPX1, SOD1, SOD2 and CAT were all increased in response to 24 h cisplatin treatment. Co-treatment with 5 µM CBD was unable to correct the mRNA expression levels of SOD2 and CAT (Fig. 4C) but decreased GPX1 and SOD1 mRNA expression levels compared to cisplatin treatment (Fig. 4C).

Effect of cisplatin and CBD treatment on mitochondria. In order to analyze the early effects of cisplatin and CBD on mitochondrial biogenesis and quality control, we estimated mitochondrial density by measuring mtDNA(mitochondrial DNA) content and we measured the mRNA expression levels of genes involved in mitochondrial biogenesis (PGC1α), fission (DRP1, FIS1), fusion (OPA1), and mitophagy (PRKN) in response to 24 h cisplatin and CBD treatments. In these conditions, there were no significant changes in mtDNA content (Fig. 5A)

or mRNA expression levels of PGC1α, FIS1, DRP1 and OPA1 (Fig. 5B-E), but we observed a dramatic ≈95% reduction in PRKN mRNA expression compared to controls (Fig. 5F). Adding 5µM CBD to the cisplatin treatment did not result in any changes in mtDNA content or mRNA expression of PGC1α, OPA1, DRP1, FIS1 and PRKN compared to cisplatin treatment alone (Fig. 5A-F). In a second step, we studied the effect of cisplatin and CBD treatments on the expression of the different mitochondrial respiratory chain complexes. As shown in Figure 6A-B, western blot quantification showed a marked increase in the content of several mitochondrial proteins in C2C12 myotubes treated with 50µM cisplatin, with significant increases in NDUFB8 (complex I, $p<0.01$), UQCRC2 (complex III, $p<0.05$) and COX4 (complex IV, $p<0.05$) that were restored to control levels by co-treatment with CBD. Finally, we studied the expression of VDAC1, which is a major mitochondrial transporter that plays a key role in ATP production and is recognized as a key protein in mitochondria-mediated apoptosis (33). Cisplatin treatment of C2C12 myotubes led to a 5-fold increase in VDAC1 protein level, which was partly corrected by CBD treatment (Fig. 6C-D). In a final step, we measured citrate synthase and COX activities. Treatment of C2C12 myotubes with 50µM cisplatin resulted in a significant ≈15% increase in citrate synthase activity (Fig. 6E, $p<0.05$) an a ≈50% increase in COX activity (Fig. 6F, $p=0.07$) that were not corrected by CBD co-treatment.

DISCUSSION

The objective of this study was to investigate whether treatment with CBD was able to prevent chemotherapy-induced skeletal muscle atrophy in a cisplatin-treated model of myotubes in culture. In a first set of experiments, we demonstrated that CBD was able to prevent cisplatin-induced apoptosis and myotube atrophy. The increased protein synthesis and decreased proteolysis induced by CBD in cisplatin-treated myotubes explain the anti-atrophic effects of CBD. In a second set of experiments, we showed that cisplatin-induced atrophy was associated with the induction of oxidative stress that was prevented by CBD co-treatment. Finally, we observed early cisplatin-induced alterations in the expression of several mitochondrial proteins involved in mitochondrial respiration and control of apoptosis, and these alterations were also prevented by CBD co-treatment.

Mitochondria plays an important role in regulating many cellular functions, including ATP production, generation of reactive oxygen species (ROS), and induction of apoptosis (34). Cells maintain optimal mitochondrial health through several pathways, including mitochondrial biogenesis, mitochondrial dynamics (fusion and fission processes shaping mitochondrial

morphology), and mitophagy (the process that removes defective mitochondria through autophagy) (35). Alterations in mitochondrial distribution, morphology and function have been reported in many conditions that lead to skeletal muscle wasting, including cachexia and sarcopenia (36, 37). Here, we analyzed the mRNA expression levels of several markers of mitochondrial dynamics in response to cisplatin and CBD treatments in myotubes in culture. We observed no major effect of cisplatin or CBD on the mRNA expression levels of genes involved in mitochondrial biogenesis (PGC1α), fusion (Opa1), and fission (DRP1, FIS1). However, there was a drastic reduction in the expression of the PRKN gene encoding the Parkin protein. This could reflect inhibition of PARKIN-dependent mitophagy, leading to an accumulation of dysfunctional mitochondria and, ultimately, muscle wasting (38). Previous studies have shown that cisplatin (and chemotherapy in general) causes a decrease in mitochondrial respiration and alterations in mitochondrial biogenesis and fusion/fission processes in models of cancer or chemotherapy, but also in cancer patients (13, 16, 18, 19). Our findings therefore seem to contradict the literature, but there are several possible explanations for this divergence. The majority of studies characterizing the effect of cisplatin on muscle atrophy were carried out *in vivo*, either in rodents or in cancer patients, and treatments were carried out over periods of several days, sometimes with tumor implantation. One limitation of our *in vitro* myotube model is that it does not represent the cellular heterogeneity found in skeletal muscle, which consists of satellite cells, myoblasts, fibro-adipogenic progenitor cells, and immune cells. Further research is needed to investigate the impact of CBD on this heterogeneity and the coordinated functioning of different cell types.

In the present study, we also documented alterations in the expression of several proteins of the mitochondrial electron transport chain (ETC). Cisplatin treatment was associated with increased protein expression of NDUFB8 (complex I), UQCRC2 (complex III), and COX4 (complex IV) that were corrected by CBD, while protein expression of SDHB (complex II) and ATP5A (complex V) was unaffected. In sarcopenia, deficient ETC activity is associated with loss of muscle mass (39). Given that normal ETC function requires proportionally balanced activities of these different complexes (40), the increased expression of NDUFB8, UQCRC2 and COX4 could reflect imbalanced ETC activity and reduced energy production. The reduced ATP content observed in cisplatin-treated myotubes and the increased level of AMPK phosphorylation (indicating energy depletion) supports this hypothesis, but further investigation is needed to fully understand the effects of cisplatin and CBD treatments on the activity of the different mitochondrial complexes and on mitochondrial respiration. One of the

key proteins that control mitochondrial function is VDAC1, which plays a crucial role in the release of ROS and in regulating apoptosis through the release of mitochondrial pro-apoptotic factors such as cytochrome C and subsequent cleavage of caspase 3 (41). Several studies have shown that the cytotoxic effect of cisplatin on cancer cell lines is associated with upregulation of VDAC1 and excessive production of ROS (16, 42). To our knowledge, our study is the first to demonstrate increased expression of VDAC1 in response to cisplatin in a model of skeletal muscle in vitro, and its correction by CBD. It is still unclear how CBD counters these mitochondrial alterations, but the answer may lie in its antioxidative properties.

Cisplatin is widely used to combat multiple types of cancers, but it has side effects such as oxidative stress in muscle cells (12, 16). Antioxidative strategies are expected to be useful in limiting oxidative stress-induced skeletal muscle damage (43). As expected, cisplatin treatment resulted in increased TBARS levels (index of lipid peroxidation) together with increased catalase activity and mRNA expression levels of several antioxidant systems (GPX1, SOD1/2, CAT) aimed at detoxifying excessive ROS production. To our knowledge, our study is the first to demonstrate the antioxidative properties of CBD in cisplatin-treated myotubes in vitro. Previous studies have shown that CBD has an antioxidant function (22) that comes from its ability to capture free radicals or transform them into less active forms. For example, CBD was shown to directly prevent the formation of superoxide radicals in a renal nephropathy model using cisplatin-treated mice (22), to reduce nitric oxide (NO) levels in the liver of doxorubicin-treated mice (22), and to suppress ROS production by chelating transition metal ions involved in the Fenton reaction (22). Note too that CBD modifies cellular redox status by modulating both the expression and enzymatic activity of antioxidant systems (22). Our results demonstrated that CBD was able to prevent the cisplatin-induced accumulation of TBARS. The fact that CBD reduced the mRNA expression of antioxidant systems (GPX1, SOD1/2, CAT) and catalase activity in response to cisplatin strongly suggests a direct effect of CBD by capturing ROS and reducing NO production in response to cisplatin, or by reducing their production by increasing the levels of antioxidants such as glutathione (22).

On top of these direct antioxidant effects, CBD also indirectly modulates redox state by interacting with several molecular targets, including the EC receptors CB1 and CB2, and PPARγ which controls the expression of antioxidant systems such as catalase and SOD2 (22). CBD is not only a PPARγ receptor agonist, but can also increase enzymatic antioxidant activities (22). CBD could also improve oxidative state by modulating the activity of the CB1 and CB2 receptors. Indeed, CB1 activation increases ROS production whereas CB2 activation

decreases ROS production (44), and it has been shown that CBD is a negative allosteric modulator of the CB1 receptor (45). Further studies are needed to fully understand which of these targets mediate the protective effect of CBD in our *in vitro* model.

Oxidative stress is one of the primary causes of skeletal muscle atrophy in several patho-physiological conditions, including muscle inactivity, muscular dystrophy, sarcopenia, and cachexia (43). Regulation of skeletal muscle mass depends on the balance between protein synthesis and degradation. Protein synthesis is mainly controlled by the Akt/mTOR (mammalian target of rapamycin) and GCN2/eIF2α pathways (46, 47). Excessive production of ROS is known to activate PERK, a key endoplasmic reticulum stress transducer of the unfolded protein response pathway (47) that activates eIF2α and inhibits protein synthesis. In skeletal muscle, excessive oxidative stress is also known to impair insulin signaling and Akt activation upstream of mTOR, which is important for controlling both protein synthesis and degradation (46). Given the drastic reduction of lipid peroxidation observed here with CBD in cisplatin-treated myotubes, it is highly conceivable that CBD helps maintain protein homeostasis by preventing excessive oxidative stress.

In summary, using a model of cultured C2C12 myotubes, we demonstrated that CBD prevented cisplatin-induced atrophy by maintaining protein homeostasis (i.e. promoting protein synthesis and limiting proteolysis) by reducing oxidative stress. In cancer patients, muscle mass is predictive of survival but also of response to chemotherapy, which makes it crucial to develop strategies for maintaining muscle mass in these patients. Cisplatin is an antineoplastic agent that is commonly used in the treatment of solid tumors such as ovarian carcinoma and in head and neck squamous cell carcinoma (HNSCC) (48). The toxicity of cisplatin is due to its DNA binding followed by single-stranded DNA breaks, but also its ability to generate oxidative stress in tumor cells. Consequently, some may consider that using CBD for its antioxidant activity could undermine the efficacy of cisplatin treatment. However, rather than reducing cisplatin toxicity, CBD was recently found to potentiate the antineoplasic effect of cisplatin in a model of HNSSC (48). Taken together, the evidence suggests that CBD could be used as an adjuvant in the treatment of cancer cachexia to help maintain muscle mass and improve patient quality of life.

GRANTS

This study was supported by the INRAE AlimH (Alimentation Humaine) Department.

CONFLICT OF INTEREST

The authors declare they have no conflict of interest.

FIGURE LEGENDS

Figure1. CBD prevents cisplatin-induced atrophy and apoptosis in C2C12 myotubes. **a)** Representative pictures of myotube morphology at 24 h of incubation. **b)** Myotube diameter of cisplatin and CBD treated cells. **c)** 48 h Myotube viability. **d)** Representative western blot showing level of cleaved caspase 3 in response to 24 h treatments. **e)** Quantification of cleaved caspase 3 level from (d). Results are expressed as mean ± sem. ** $p<0.01$ vs. CTL, ◆ $p<0.05$ vs. CIS, ◆◆ $p<0.01$ vs. CIS, ## $p<0.01$ between CBD conditions.

Figure 2. CBD prevents cisplatin-induced decrease in protein synthesis in C2C12 myotubes. **a)** Representative western blot of puromycin incorporation and the phosphorylation state of Akt (Ser473-phospho-Akt), S6K (Thr389-phospho-S6K) and eIF2α (Ser51-phospho- eIF2α) in response to 24 h treatment with cisplatin and CBD. Quantification of (**b**) puromycin incorporation signal, (**c**) phospho-S6K, (**d**) phospho-Akt, and (**e**) phospho- eIF2α levels. Results are expressed as mean ± sem. ** $p<0.01$ vs. CTL, * $p<0.05$ vs. CTL, ◆ $p<0.05$ vs. CIS, ◆◆ $p<0.01$ vs. CIS, ## $p<0.01$ between CBD conditions.

Figure 3. CBD prevents cisplatin-induced proteolysis and atrogene expression. **a)** Representative western blot showing the level of protein poly-ubiquitination in response to 24 h treatment with cisplatin and CBD. **b)** Quantification of total protein polyubiquitination from (a). **c)** Real-time PCR quantification of *Atrogin/MAFbx* mRNA expression. **d)** Real-time PCR quantification of *MuRF1* mRNA expression. Results are expressed as mean ± sem. ** $p<0.01$ vs. CTL, * $p<0.05$ vs. CTL, ◆ $p<0.05$ vs. CIS.

Figure 4. CBD prevents cisplatin-induced oxidative stress. **a)** TBARS content in C2C12 myotubes treated for 24 h with cisplatin and CBD. **b)** Catalase activity. **c)** Real-time PCR quantification of *Gpx1, Sod1, Sod2 and Cat* mRNA expression. Results are expressed as mean ± sem. ** $p<0.01$ vs. CTL, * $p<0.05$ vs. CTL, ◆ $p<0.05$ vs. CIS. ◆◆ $p<0.01$ vs. CIS.

Figure 5. Effect of cisplatin and CBD co-treatment on C2C12 myotube mitochondrial dynamics. **a)** Real-time PCR quantification of mtDNA expression in C2C12 myotubes treated for 24 h with cisplatin and CBD. Real-time PCR quantification of *Pgc1alpha* **(b)**, *Fis1* **(c),**

Drp1 **(d)**, *Opa1* **(e)**, and *Prkn* **(f)** mRNA expression. Results are expressed as mean ± sem. ** $p<0.01$ vs. CTL.

Figure 6. Effect of cisplatin and CBD on C2C12 myotube mitochondrial protein content and activity. **a)** Representative western blot showing the expression levels of proteins related to mitochondrial oxidative phosphorylation (OXPHOS) in C2C12 myotubes treated for 24 h with cisplatin and CBD. **b)** Quantification of several subunits of each mitochondrial complex from (a). **c)** Representative western blot showing the expression levels of VDAC1. **d)** Quantification of VDAC1 protein content from (c). (**e**) Citrate synthase activity and (**f**) COX activity. Results are expressed as mean ± sem. ** $p<0.01$ vs. CTL, * $p<0.05$ vs. CTL, ◆ $p<0.05$ vs. CIS. ◆◆ $p<0.01$ vs. CIS.

Table 1. List of primers used for real-time qPCR

Gene name	**5'- Sense primer -3'**	**5'- Antisense primer -3'**
Actin (DNA primer)	TACAGCTTCACCACCACAGC	AAGGAAGGCTGGAAAAGAGC
Atrogin/MAFBx	AAGCTTGTGCGATGTTACCCA	CACGGATGGTCAGTGCCCTT
Cat	CCTTCAAGTTGGTTAATGCAGA	CAAGTTTTTGATGCCCTGGT
Drp1	TGCCTCAGATCGTCGTAGTG	TGACCACACCAGTTCCTCTG
Fis1	GCCTGGTTCGAAGCAAATAC	CACGGCCAGGTAGAAGACAT
Gpx1	GTGAGCCTGGGCTCCCTGCG	ACTTGAGGGAATTCAGAATC
MuRF1	AGGTGTCAGCGCAAAGCAGT	CCTCCTTTGTCCTCTTGCTG
Nd1 (DNA primer)	GGCCCCCTTCGACCTGACAGA	TAACGCGAATGGGCCGGCTG
Opa1	GATGACACGCTCTCCAGTGAAG	CTCGGGGCTAACAGTACAACC
Ppargc1a	GAAGTGGTGTAGCGACCAATC	AATGAGGGCAATCCGTCTTCA
Prkn	ATTCCAAACCGGATGAGTGG	TTGTCTGAGGTTGGGTGTGC
Sod1	CAGGACCTCATTTTAATCCTCAC	TGCCCAGGTCTCCAACAT
Sod2	GACCTGCCTTACGACTAT	TACTTCTCCTCGGTGACG
18S	CGGCTACCACATCCAAGGAA	GCTGGAATTACCGCGGCT

REFERENCES

1. **Fearon K, Strasser F, Anker SD, Bosaeus I, Bruera E, Fainsinger RL, Jatoi A, Loprinzi C, MacDonald N, Mantovani G, Davis M, Muscaritoli M, Ottery F, Radbruch L, Ravasco P, Walsh D, Wilcock A, Kaasa S, and Baracos VE**. Definition and classification of cancer cachexia: an international consensus. *Lancet Oncol* 12: 489-495, 2011.
2. **Anker MS, Holcomb R, Muscaritoli M, von Haehling S, Haverkamp W, Jatoi A, Morley JE, Strasser F, Landmesser U, Coats AJS, and Anker SD**. Orphan disease status of cancer cachexia in the USA and in the European Union: a systematic review. *Journal of cachexia, sarcopenia and muscle* 10: 22-34, 2019.
3. **Pin F, Couch ME, and Bonetto A**. Preservation of muscle mass as a strategy to reduce the toxic effects of cancer chemotherapy on body composition. *Curr Opin Support Palliat Care* 12: 420-426, 2018.
4. **Andreyev HJ, Norman AR, Oates J, and Cunningham D**. Why do patients with weight loss have a worse outcome when undergoing chemotherapy for gastrointestinal malignancies? *Eur J Cancer* 34: 503-509, 1998.
5. **Persson C, and Glimelius B**. The relevance of weight loss for survival and quality of life in patients with advanced gastrointestinal cancer treated with palliative chemotherapy. *Anticancer Res* 22: 3661-3668, 2002.
6. **Dahele M, Skipworth RJ, Wall L, Voss A, Preston T, and Fearon KC**. Objective physical activity and self-reported quality of life in patients receiving palliative chemotherapy. *J Pain Symptom Manage* 33: 676-685, 2007.
7. **Ross PJ, Ashley S, Norton A, Priest K, Waters JS, Eisen T, Smith IE, and O'Brien ME**. Do patients with weight loss have a worse outcome when undergoing chemotherapy for lung cancers? *British journal of cancer* 90: 1905-1911, 2004.
8. **Siddiqui JA, Pothuraju R, Jain M, Batra SK, and Nasser MW**. Advances in cancer cachexia: Intersection between affected organs, mediators, and pharmacological interventions. *Biochim Biophys Acta Rev Cancer* 1873: 188359, 2020.
9. **Roeland EJ, Bohlke K, Baracos VE, Bruera E, Del Fabbro E, Dixon S, Fallon M, Herrstedt J, Lau H, Platek M, Rugo HS, Schnipper HH, Smith TJ, Tan W, and Loprinzi CL**. Management of Cancer Cachexia: ASCO Guideline. *J Clin Oncol* 38: 2438-2453, 2020.
10. **Klassen O, Schmidt ME, Ulrich CM, Schneeweiss A, Potthoff K, Steindorf K, and Wiskemann J**. Muscle strength in breast cancer patients receiving different treatment regimes. *Journal of cachexia, sarcopenia and muscle* 8: 305-316, 2017.
11. **Lin KY, Cheng HC, Yen CJ, Hung CH, Huang YT, Yang HL, Cheng WT, and Tsai KL**. Effects of Exercise in Patients Undergoing Chemotherapy for Head and Neck Cancer: A Pilot Randomized Controlled Trial. *Int J Environ Res Public Health* 18: 2021.
12. **Sakai H, Sagara A, Arakawa K, Sugiyama R, Hirosaki A, Takase K, Jo A, Sato K, Chiba Y, Yamazaki M, Matoba M, and Narita M**. Mechanisms of cisplatin-induced muscle atrophy. *Toxicol Appl Pharmacol* 278: 190-199, 2014.
13. **Hao E, Mukhopadhyay P, Cao Z, Erdelyi K, Holovac E, Liaudet L, Lee WS, Hasko G, Mechoulam R, and Pacher P**. Cannabidiol Protects against Doxorubicin-Induced Cardiomyopathy by Modulating Mitochondrial Function and Biogenesis. *Mol Med* 21: 38-45, 2015.
14. **Halle JL, Pena GS, Paez HG, Castro AJ, Rossiter HB, Visavadiya NP, Whitehurst MA, and Khamoui AV**. Tissue-specific dysregulation of mitochondrial respiratory capacity and coupling control in colon-26 tumor-induced cachexia. *American journal of physiology Regulatory, integrative and comparative physiology* 317: R68-R82, 2019.

15. **Brown JL, Rosa-Caldwell ME, Lee DE, Blackwell TA, Brown LA, Perry RA, Haynie WS, Hardee JP, Carson JA, Wiggs MP, Washington TA, and Greene NP**. Mitochondrial degeneration precedes the development of muscle atrophy in progression of cancer cachexia in tumour-bearing mice. *Journal of cachexia, sarcopenia and muscle* 8: 926-938, 2017.
16. **Conte E, Bresciani E, Rizzi L, Cappellari O, De Luca A, Torsello A, and Liantonio A**. Cisplatin-Induced Skeletal Muscle Dysfunction: Mechanisms and Counteracting Therapeutic Strategies. *International journal of molecular sciences* 21: 2020.
17. **Gilliam LA, Moylan JS, Patterson EW, Smith JD, Wilson AS, Rabbani Z, and Reid MB**. Doxorubicin acts via mitochondrial ROS to stimulate catabolism in C2C12 myotubes. *American journal of physiology Cell physiology* 302: C195-202, 2012.
18. **Min K, Kwon OS, Smuder AJ, Wiggs MP, Sollanek KJ, Christou DD, Yoo JK, Hwang MH, Szeto HH, Kavazis AN, and Powers SK**. Increased mitochondrial emission of reactive oxygen species and calpain activation are required for doxorubicin-induced cardiac and skeletal muscle myopathy. *The Journal of physiology* 593: 2017-2036, 2015.
19. **Argiles JM, Lopez-Soriano FJ, and Busquets S**. Muscle wasting in cancer: the role of mitochondria. *Current opinion in clinical nutrition and metabolic care* 18: 221-225, 2015.
20. **Bowen TS, Schuler G, and Adams V**. Skeletal muscle wasting in cachexia and sarcopenia: molecular pathophysiology and impact of exercise training. *Journal of cachexia, sarcopenia and muscle* 6: 197-207, 2015.
21. **Mazier W, Saucisse N, Gatta-Cherifi B, and Cota D**. The Endocannabinoid System: Pivotal Orchestrator of Obesity and Metabolic Disease. *Trends in endocrinology and metabolism: TEM* 26: 524-537, 2015.
22. **Atalay S, Jarocka-Karpowicz I, and Skrzydlewska E**. Antioxidative and Anti-Inflammatory Properties of Cannabidiol. *Antioxidants (Basel)* 9: 2019.
23. **Lipina C, Irving AJ, and Hundal HS**. Mitochondria: a possible nexus for the regulation of energy homeostasis by the endocannabinoid system? *American journal of physiology Endocrinology and metabolism* 307: E1-13, 2014.
24. **Iannotti FA, Silvestri C, Mazzarella E, Martella A, Calvigioni D, Piscitelli F, Ambrosino P, Petrosino S, Czifra G, Biro T, Harkany T, Taglialatela M, and Di Marzo V**. The endocannabinoid 2-AG controls skeletal muscle cell differentiation via CB1 receptor-dependent inhibition of Kv7 channels. *Proceedings of the National Academy of Sciences of the United States of America* 111: E2472-2481, 2014.
25. **Le Bacquer O, Lanchais K, Combe K, Van Den Berghe L, and Walrand S**. Acute rimonabant treatment promotes protein synthesis in C2C12 myotubes through a CB1-independent mechanism. *Journal of cellular physiology* 236: 2669-2683, 2021.
26. **Iannotti FA, Pagano E, Guardiola O, Adinolfi S, Saccone V, Consalvi S, Piscitelli F, Gazzerro E, Busetto G, Carrella D, Capasso R, Puri PL, Minchiotti G, and Di Marzo V**. Genetic and pharmacological regulation of the endocannabinoid CB1 receptor in Duchenne muscular dystrophy. *Nature communications* 9: 3950, 2018.
27. **Iannotti FA, Pagano E, Moriello AS, Alvino FG, Sorrentino NC, D'Orsi L, Gazzerro E, Capasso R, De Leonibus E, De Petrocellis L, and Di Marzo V**. Effects of non-euphoric plant cannabinoids on muscle quality and performance of dystrophic mdx mice. *British journal of pharmacology* 2018.
28. **Le Bacquer O, Salles J, Piscitelli F, Sanchez P, Martin V, Montaurier C, Di Marzo V, and Walrand S**. Alterations of the endocannabinoid system and circulating and peripheral tissue levels of endocannabinoids in sarcopenic rats. *Journal of cachexia, sarcopenia and muscle* 13: 662-676, 2022.
29. **Fajardo L, Sanchez P, Salles J, Rigaudiere JP, Patrac V, Caspar-Bauguil S, Bergoglgio C, Moro C, Walrand S, and Le Bacquer O**. Inhibition of the endocannabinoid system reverses obese phenotype in aged mice and partly restores skeletal muscle function. *American journal of physiology Endocrinology and metabolism* 2023.
30. **Kis B, Ifrim FC, Buda V, Avram S, Pavel IZ, Antal D, Paunescu V, Dehelean CA, Ardelean F, Diaconeasa Z, Soica C, and Danciu C**. Cannabidiol-from Plant to Human Body: A Promising Bioactive Molecule with Multi-Target Effects in Cancer. *International journal of molecular sciences* 20: 2019.

31. **Bielawiec P, Harasim-Symbor E, Konstantynowicz-Nowicka K, Sztolsztener K, and Chabowski A**. Chronic Cannabidiol Administration Attenuates Skeletal Muscle De Novo Ceramide Synthesis Pathway and Related Metabolic Effects in a Rat Model of High-Fat Diet-Induced Obesity. *Biomolecules* 10: 2020.
32. **Yu W, Chen Y, Dubrulle J, Stossi F, Putluri V, Sreekumar A, Putluri N, Baluya D, Lai SY, and Sandulache VC**. Cisplatin generates oxidative stress which is accompanied by rapid shifts in central carbon metabolism. *Scientific reports* 8: 4306, 2018.
33. **Shoshan-Barmatz V, Shteinfer-Kuzmine A, and Verma A**. VDAC1 at the Intersection of Cell Metabolism, Apoptosis, and Diseases. *Biomolecules* 10: 2020.
34. **Pfanner N, Warscheid B, and Wiedemann N**. Mitochondrial proteins: from biogenesis to functional networks. *Nature reviews Molecular cell biology* 20: 267-284, 2019.
35. **Leduc-Gaudet JP, Hussain SNA, Barreiro E, and Gouspillou G**. Mitochondrial Dynamics and Mitophagy in Skeletal Muscle Health and Aging. *International journal of molecular sciences* 22: 2021.
36. **Carson JA, Hardee JP, and VanderVeen BN**. The emerging role of skeletal muscle oxidative metabolism as a biological target and cellular regulator of cancer-induced muscle wasting. *Seminars in cell & developmental biology* 54: 53-67, 2016.
37. **Chabi B, Ljubicic V, Menzies KJ, Huang JH, Saleem A, and Hood DA**. Mitochondrial function and apoptotic susceptibility in aging skeletal muscle. *Aging cell* 7: 2-12, 2008.
38. **Peker N, Sharma M, and Kambadur R**. Parkin deficiency exacerbates fasting-induced skeletal muscle wasting in mice. *NPJ Parkinsons Dis* 8: 159, 2022.
39. **Bua EA, McKiernan SH, Wanagat J, McKenzie D, and Aiken JM**. Mitochondrial abnormalities are more frequent in muscles undergoing sarcopenia. *J Appl Physiol (1985)* 92: 2617-2624, 2002.
40. **Miro O, Casademont J, Casals E, Perea M, Urbano-Marquez A, Rustin P, and Cardellach F**. Aging is associated with increased lipid peroxidation in human hearts, but not with mitochondrial respiratory chain enzyme defects. *Cardiovasc Res* 47: 624-631, 2000.
41. **Camara AKS, Zhou Y, Wen PC, Tajkhorshid E, and Kwok WM**. Mitochondrial VDAC1: A Key Gatekeeper as Potential Therapeutic Target. *Frontiers in physiology* 8: 460, 2017.
42. **Luo L, Xiong Y, Jiang N, Zhu X, Wang Y, Lv Y, and Xie Y**. VDAC1 as a target in cisplatin anti-tumor activity through promoting mitochondria fusion. *Biochemical and biophysical research communications* 560: 52-58, 2021.
43. **Lian D, Chen MM, Wu H, Deng S, and Hu X**. The Role of Oxidative Stress in Skeletal Muscle Myogenesis and Muscle Disease. *Antioxidants (Basel)* 11: 2022.
44. **Han KH, Lim S, Ryu J, Lee CW, Kim Y, Kang JH, Kang SS, Ahn YK, Park CS, and Kim JJ**. CB1 and CB2 cannabinoid receptors differentially regulate the production of reactive oxygen species by macrophages. *Cardiovasc Res* 84: 378-386, 2009.
45. **Laprairie RB, Bagher AM, Kelly ME, and Denovan-Wright EM**. Cannabidiol is a negative allosteric modulator of the cannabinoid CB1 receptor. *British journal of pharmacology* 172: 4790-4805, 2015.
46. **Saxton RA, and Sabatini DM**. mTOR Signaling in Growth, Metabolism, and Disease. *Cell* 168: 960-976, 2017.
47. **Donnelly N, Gorman AM, Gupta S, and Samali A**. The eIF2alpha kinases: their structures and functions. *Cellular and molecular life sciences : CMLS* 70: 3493-3511, 2013.
48. **Go YY, Kim SR, Kim DY, Chae SW, and Song JJ**. Cannabidiol enhances cytotoxicity of anti-cancer drugs in human head and neck squamous cell carcinoma. *Scientific reports* 10: 20622, 2020.

Figure 1

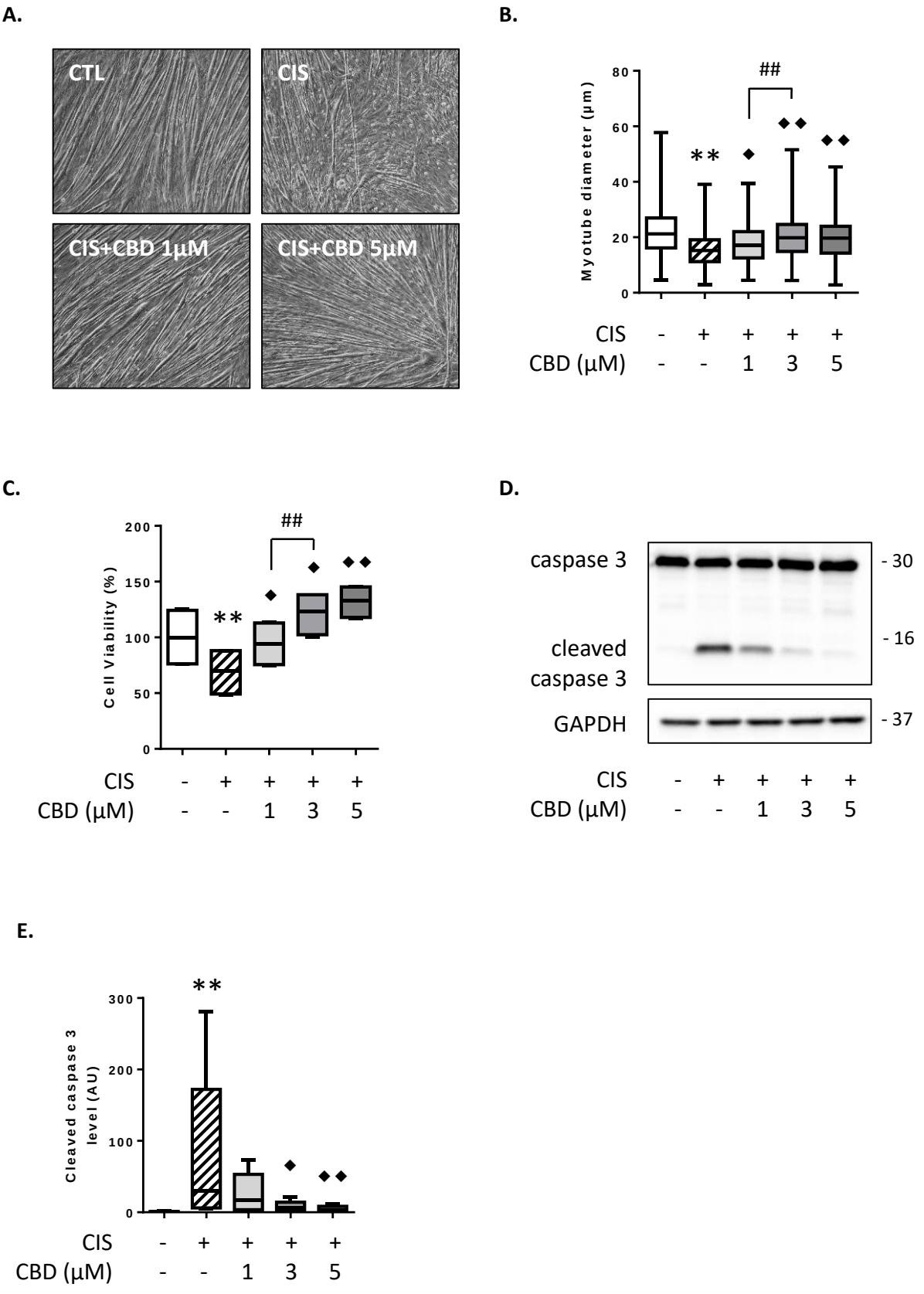
A.
CTL
CIS
CIS+CBD 1µM
CIS+CBD 5µM
B.
Myotube diameter (µm)
80
60
40
20
0
**
##
CIS - + + + +
CBD (µM) - - 1 3 5
C.
Cell Viability (%)
200
150
100
50
0
**
##
CIS - + + + +
CBD (µM) - - 1 3 5
D.
caspase 3
cleaved caspase 3
GAPDH
- 30
- 16
- 37
CIS - + + + +
CBD (µM) - - 1 3 5
E.
Cleaved caspase 3 level (AU)
300
200
100
0
**
CIS - + + + +
CBD (µM) - - 1 3 5

Figure 2

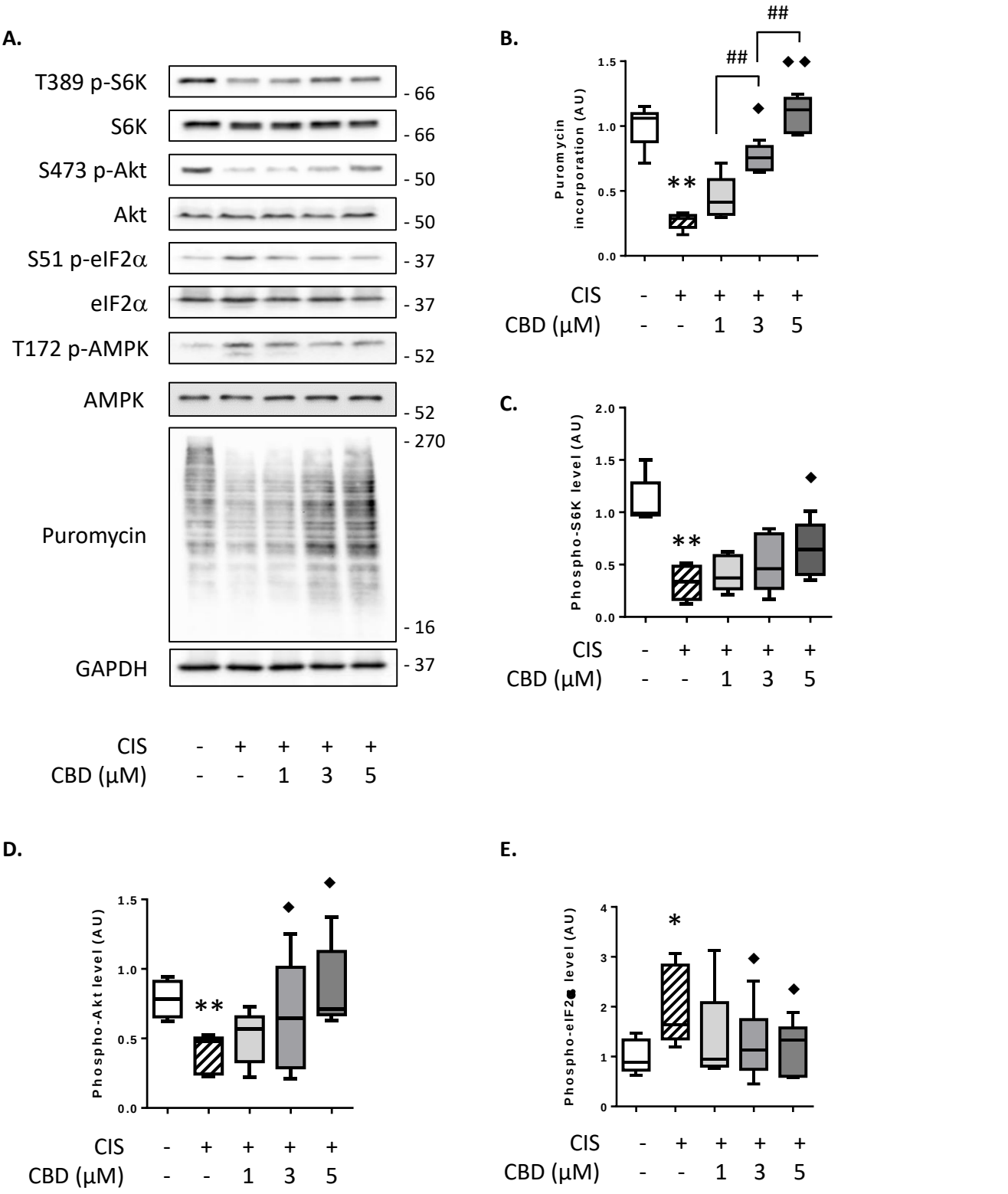
A.
T389 p-S6K
S6K
S473 p-Akt
Akt
S51 p-eIF2α
eIF2α
T172 p-AMPK
AMPK
Puromycin
GAPDH
- 66
- 66
- 50
- 50
- 37
- 37
- 52
- 52
- 270
- 16
- 37
CIS - + + + +
CBD (μM) - - 1 3 5
B.
Puromycin incorporation (AU)
##
##
**
CIS - + + + +
CBD (μM) - - 1 3 5
C.
Phospho-S6K level (AU)
**
CIS - + + + +
CBD (μM) - - 1 3 5
D.
Phospho-Akt level (AU)
**
CIS - + + + +
CBD (μM) - - 1 3 5
E.
Phospho-eIF2α level (AU)
*
CIS - + + + +
CBD (μM) - - 1 3 5

Figure 3

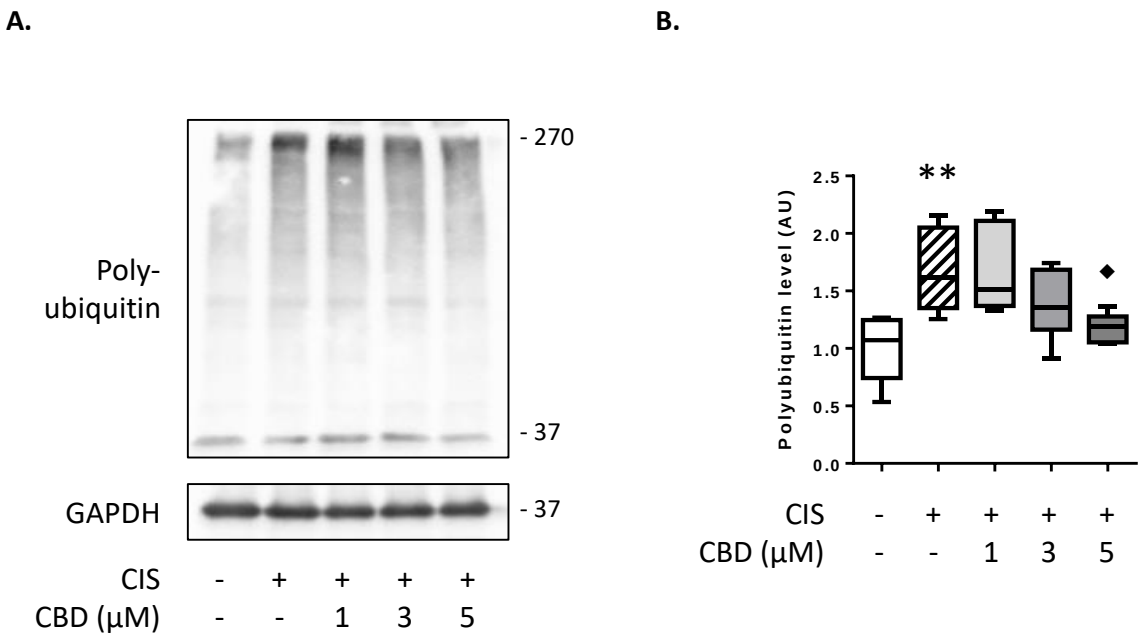
A.
Poly-
ubiquitin
- 270
- 37
GAPDH
- 37
CIS - + + + +
CBD (µM) - - 1 3 5
B.
Polyubiquitin level (AU)
2.5
2.0
1.5
1.0
0.5
0.0
**
CIS - + + + +
CBD (µM) - - 1 3 5

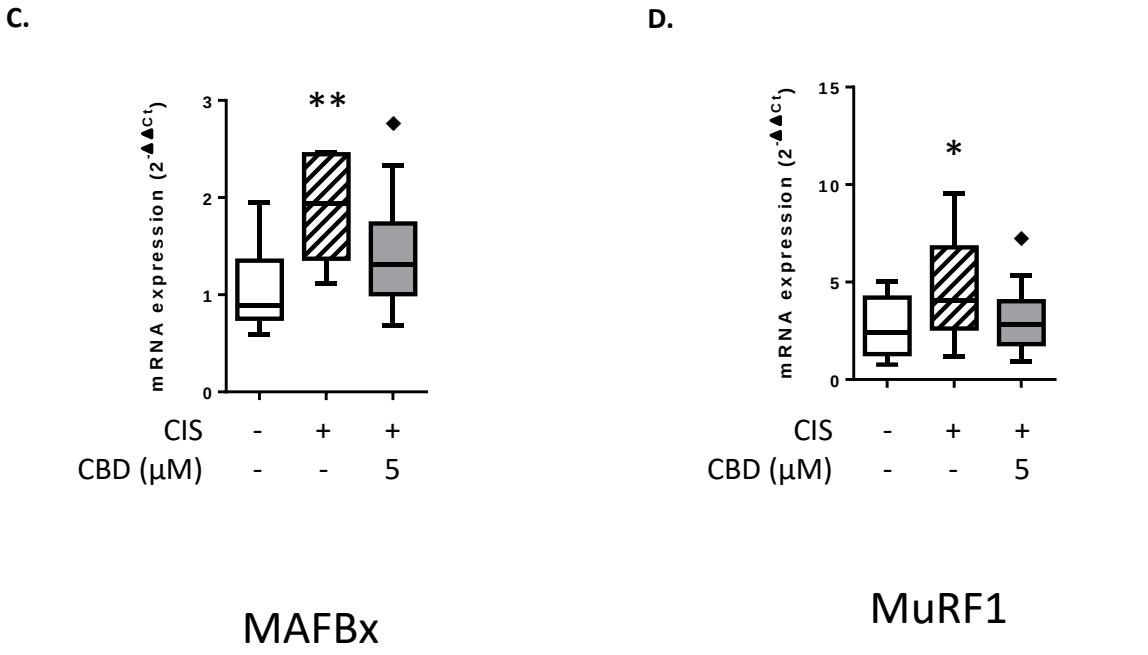
C.
mRNA expression (2-ΔΔCt)
3
2
1
0
**
CIS - + +
CBD (µM) - - 5
MAFBx
D.
mRNA expression (2-ΔΔCt)
15
10
5
0
*
CIS - + +
CBD (µM) - - 5
MuRF1

Figure 4

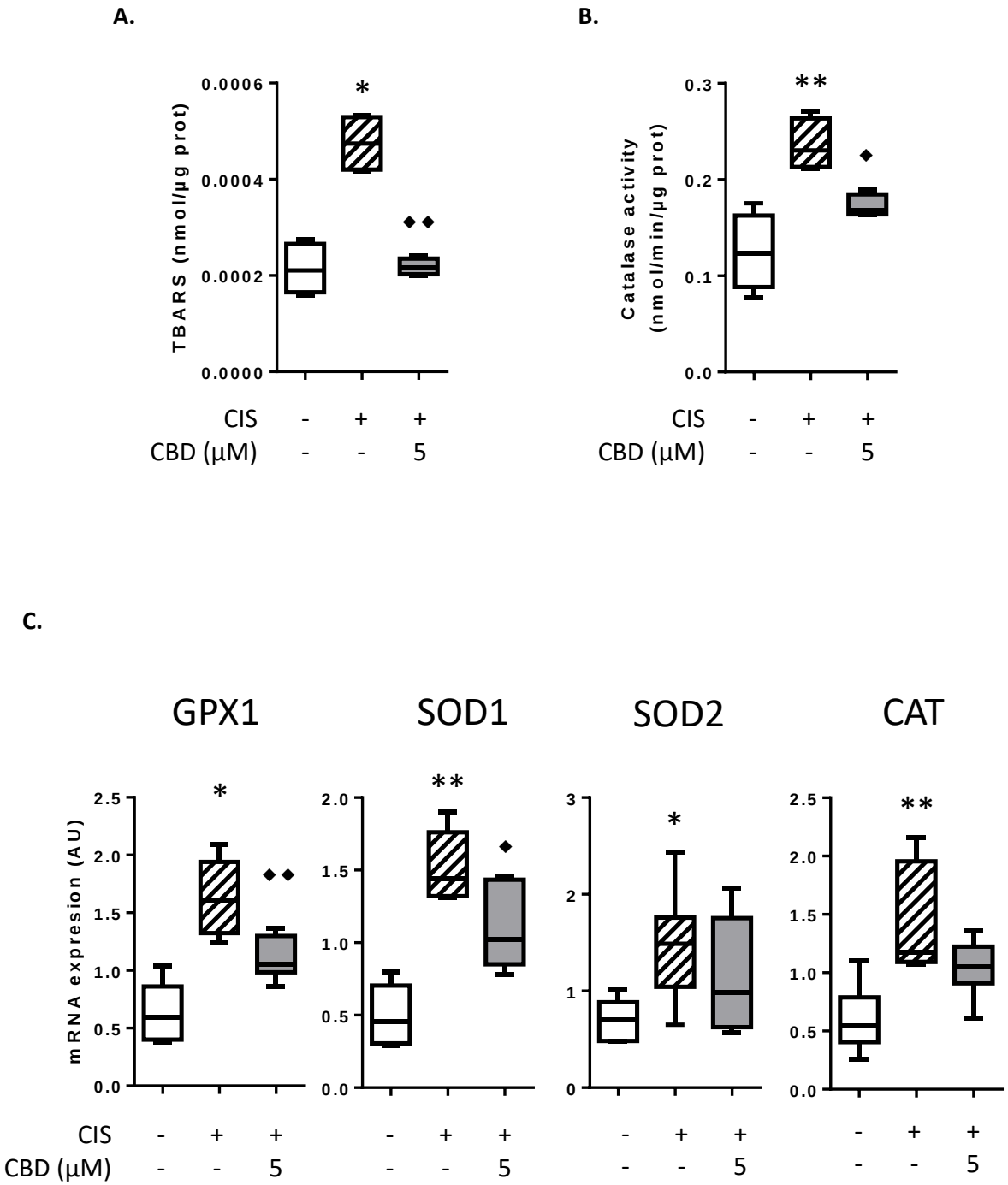
A.
TBARS (nmol/µg prot)
0.0006
0.0004
0.0002
0.0000
*
CIS - + +
CBD (µM) - - 5
B.
Catalase activity (nmol/min/µg prot)
0.3
0.2
0.1
0.0
**
CIS - + +
CBD (µM) - - 5
C.
GPX1
SOD1
SOD2
CAT
mRNA expresion (AU)
2.5
2.0
1.5
1.0
0.5
0.0
*
**
*
**
CIS - + +
CBD (µM) - - 5

Figure 5

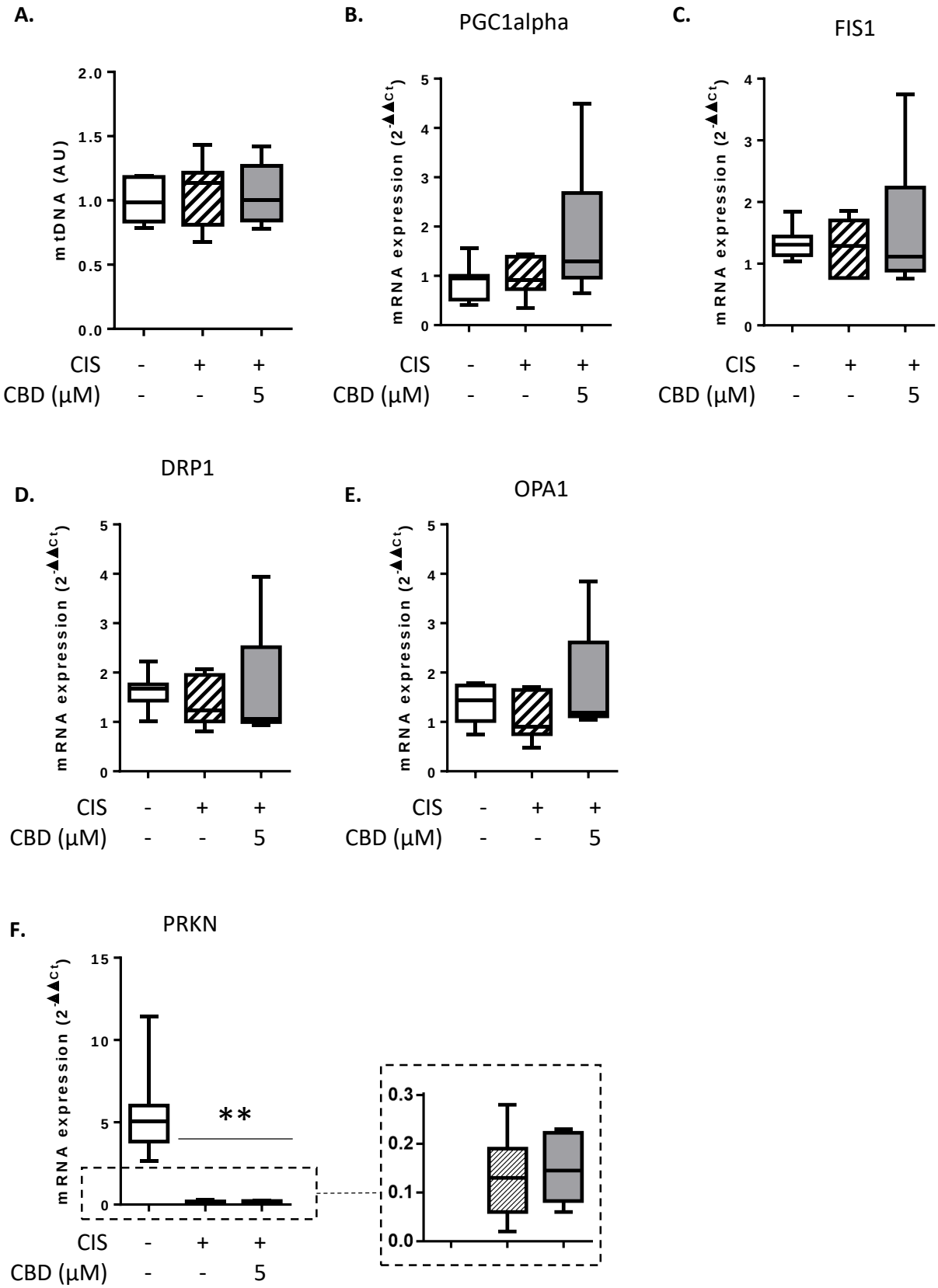
A.
mtDNA (AU)
2.0
1.5
1.0
0.5
0.0
CIS - + +
CBD (µM) - - 5
B.
PGC1alpha
mRNA expression (2-ΔΔCt)
5
4
3
2
1
0
CIS - + +
CBD (µM) - - 5
C.
FIS1
mRNA expression (2-ΔΔCt)
4
3
2
1
0
CIS - + +
CBD (µM) - - 5
D.
DRP1
mRNA expression (2-ΔΔCt)
5
4
3
2
1
0
CIS - + +
CBD (µM) - - 5
E.
OPA1
mRNA expression (2-ΔΔCt)
5
4
3
2
1
0
CIS - + +
CBD (µM) - - 5
F.
PRKN
mRNA expression (2-ΔΔCt)
15
10
5
0
**
0.3
0.2
0.1
0.0
CIS - + +
CBD (µM) - - 5

Figure 6

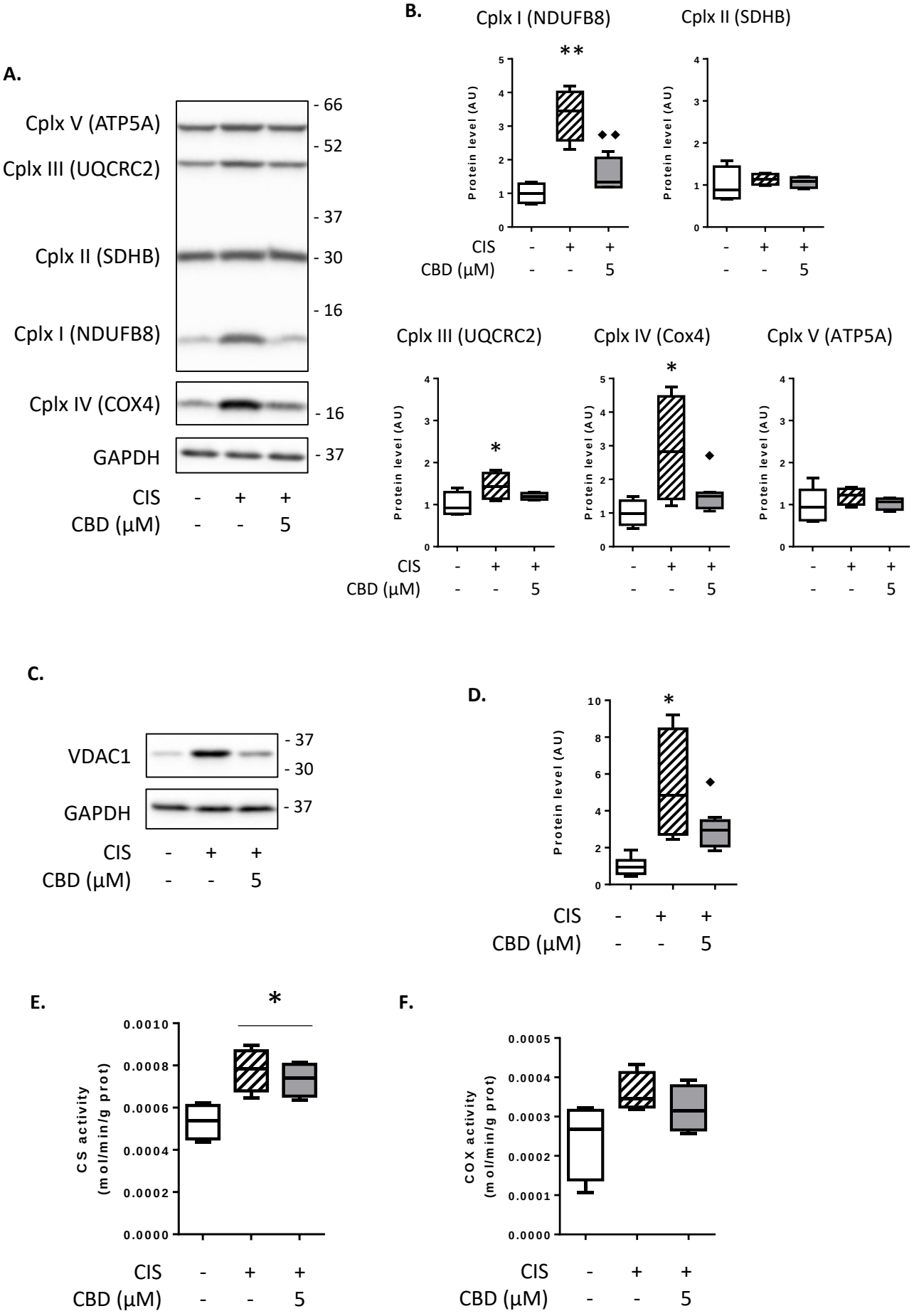
A.
Cplx V (ATP5A)
Cplx III (UQCRC2)
Cplx II (SDHB)
Cplx I (NDUFB8)
Cplx IV (COX4)
GAPDH
66
52
37
30
16
16
37
CIS - + +
CBD (µM) - - 5
B.
Cplx I (NDUFB8)
Cplx II (SDHB)
Cplx III (UQCRC2)
Cplx IV (Cox4)
Cplx V (ATP5A)
Protein level (AU)
**
*
*
*
◆◆
◆
CIS - + +
CBD (µM) - - 5
C.
VDAC1
GAPDH
37
30
37
CIS - + +
CBD (µM) - - 5
D.
Protein level (AU)
*
◆
CIS - + +
CBD (µM) - - 5
E.
CS activity (mol/min/g prot)
*
0.0010
0.0008
0.0006
0.0004
0.0002
0.0000
CIS - + +
CBD (µM) - - 5
F.
COX activity (mol/min/g prot)
0.0005
0.0004
0.0003
0.0002
0.0001
0.0000
CIS - + +
CBD (µM) - - 5